



**HAL**  
open science

# Synthesis and characterization of phenolic resins based on pyrolysis bio-oil separated by fractional condensation and water extraction

J. Xu, N. Brodu, M. Mignot, B. Youssef, B. Taouk

► **To cite this version:**

J. Xu, N. Brodu, M. Mignot, B. Youssef, B. Taouk. Synthesis and characterization of phenolic resins based on pyrolysis bio-oil separated by fractional condensation and water extraction. *Biomass and Bioenergy*, 2022, 159, pp.106393. 10.1016/j.biombioe.2022.106393 . hal-03616765

**HAL Id: hal-03616765**

**<https://hal.science/hal-03616765v1>**

Submitted on 22 Jul 2024

**HAL** is a multi-disciplinary open access archive for the deposit and dissemination of scientific research documents, whether they are published or not. The documents may come from teaching and research institutions in France or abroad, or from public or private research centers.

L'archive ouverte pluridisciplinaire **HAL**, est destinée au dépôt et à la diffusion de documents scientifiques de niveau recherche, publiés ou non, émanant des établissements d'enseignement et de recherche français ou étrangers, des laboratoires publics ou privés.



Distributed under a Creative Commons Attribution - NonCommercial 4.0 International License



10 **Abstract**

11

12 The combination of fractional condensation and water extraction methods is proposed  
13 to produce phenol rich beech wood pyrolysis bio-oil fractions, which have great  
14 potential to replace petroleum-based phenol in polymerization of novolac resin. The  
15 polymerization of model phenol acetaldehyde (MPA) resins, mimic acetaldehyde  
16 (mimic) resin which base on the composition of phenol compounds in bio-oil, bio-oil  
17 acetaldehyde (BOA) resins were studied. MPA and mimic resins were used to  
18 compare with the BOA resin to determine the feasibility of using bio-oil. Bisphenol A  
19 type epoxy resin (DGEBA) was used, for the first time, as a formaldehyde-free cross-  
20 linker for bio-oil based novolac resins. The kinetic parameters of the curing reaction  
21 with model-free methods were obtained using data from a differential scanning  
22 calorimeter (DSC). The BOA resin showed curing activation energy that was close to  
23 that of the phenol-acetaldehyde (PA) resin (95.5 and 94.9 kJ/mol by Kissinger-  
24 methods). The physicochemical and thermal properties of the novolac resins before  
25 and after curing are compared, and the potential of treated bio-oil products to  
26 effectively replace commercial phenols is demonstrated.

27

28 **Keywords:** Pyrolysis bio-oil novolac resin; Fractional condensation; Water extraction;  
29 DGEBA epoxy resin; Curing kinetics.

30 **Abbreviations:**

- 31 ATR-FTIR: Attenuated total reflection Fourier-transform infrared spectroscopy
- 32 BOA: bio-oil acetaldehyde resin
- 33 BPF: bio-oil phenol formaldehyde resin
- 34 **DCM: dichloromethane**
- 35 DGEBA: Bisphenol A type epoxy resin
- 36 DPA: 2,6-dimethylphenol acetaldehyde resin
- 37 DSC: Differential scanning calorimeter
- 38 DTG: Derivative thermogravimetry
- 39 EGA: 4-ethylguaiacol acetaldehyde resin
- 40 GC-FID: Gas chromatography with flame ionization detector
- 41 GC-MS: Gas chromatograph-mass spectrometer instrument
- 42 GPC: Gel permeation chromatography
- 43 HMTA: Hexamethylenetetramine
- 44 HPLC: High-performance liquid chromatography
- 45 **KOH: potassium hydroxide**
- 46  **$M_w$ : average molecular weight**
- 47  **$M_n$ : number average molecular weight**
- 48 MCA: m-cresol acetaldehyde resin
- 49 Mimic: mimic phenol acetaldehyde resin
- 50 MPA: model phenol acetaldehyde resin
- 51 OCA: o-cresol acetaldehyde resin
- 52 OILS, OIL1, OIL2 and **OIL3**: pyrolysis oil products from the single condenser and
- 53 fractional condensation system (the first, second and **third condenser**, respectively)

- 54 OILSA, OIL1A, OIL2A, OILSWIA, OIL1WIA, and OIL2WIA: bio-oil acetaldehyde
- 55 resin using various bio-oil products
- 56 OILSWI, OIL1WI, and OIL2WI: water-insoluble fractions of bio-oil products
- 57 PA: phenol acetaldehyde resin
- 58 PF: phenol formaldehyde resin
- 59 PHMF: phenol–hydroxymethylfurfural resin
- 60 **TPP: triphenylphosphine**
- 61 TGA: Thermogravimetric analysis

## 62        **1. Introduction**

63        The pyrolysis of biomass like beech wood is one of the pivotal conversion pathways  
64        used to obtain bio-oils from biomass in an eco-friendly and cost-effective way [1].  
65        Bio-oil is a mixture containing over 400 different chemical compounds, including  
66        carboxylic acids, phenols, ketones, esters, alcohols, sugars, aldehydes, furans, amides,  
67        alkenes, and alkanes, which lead to wide potential applications in various fields [2, 3].  
68        For instance, the main applications of bio-oils include their use as fuels, a source of  
69        chemicals, binders, functional carbon materials, etc. [4]. Since the oxygen-containing  
70        organics in bio-oil, including an abundance of simple phenols and oligomeric  
71        polyphenols, are reactive towards polymerization, they can be applied as a substitute  
72        for fossil phenols to produce such resins [1].

73        Since the discovery of phenol-formaldehyde (PF) resins, recognized as the  
74        cornerstone of the plastics industry in the early twentieth century [5], the phenolic  
75        resin has become an irreplaceable material that can be used in selective high  
76        technology applications offering high reliability under severe circumstances [6]. It has  
77        been widely used in electronics, adhesives, carbon foams, molding compounds,  
78        thermal insulation materials, and composite materials among others, due to its low  
79        cost, thermostability, and chemical durability [7]. **However, traditional non-renewable**  
80        **petroleum-based phenol and formaldehyde continue to have unfavorable effects on**  
81        **the environment and human health. In recent years, it has become a trend to partially**  
82        **or completely substitutes raw materials (phenol and formaldehyde) with sustainable**  
83        **and environmentally friendly materials in the synthesis process [7, 8].**

84        Under this premise, it is proposed to replace the phenol in **commercial phenolic resin**  
85        with the phenol fraction from bio-oils. **The potential of pyrolysis products for use in**  
86        **phenolic resins is not a new concept, but the efficient and cost-effective reduction of**

87 this to practice has been an elusive goal over many years [9]. According to the  
88 complexity of the chemical family in bio-oil, a wide variety of phenolic compounds  
89 will also complicate the polymerization reaction. Thus, there is still a need for a  
90 process designed to extract a phenolic composition from such oils which is capable of  
91 using as efficiently as petroleum-based phenols in the formation of phenol-  
92 formaldehyde resins and which is less expensive to produce [10]. Since pyrolysis oil  
93 consists of diverse compound groups having a large range of dew points, fractional  
94 condensation can be a simpler, lower cost, and more efficient approach to produce a  
95 phenol-rich liquid products compared to untreated oil [11, 12]. The high-temperature  
96 fraction mainly includes phenolic compounds and sugars. To separate the phenolic  
97 compounds and sugars, the water extraction method has been proposed [13, 14].  
98 Sugars can be separated efficiently in the water-soluble fraction, whereas phenolics  
99 remain in the water-insoluble fraction. In our previous work, the thermal stability of  
100 water insoluble fractions from pyrolysis oils at room temperature is qualitatively  
101 better than crude oil implying a good shelf life for the extract oils[15].

102 There are two types of phenolic resins, i.e., novolac and resol, which are synthesized  
103 by acid or base-catalyzed reactions between phenols and aldehydes. Cheng et al. [16]  
104 used the direct bio-oil obtained from Eastern white pine to partly replace phenol (0%  
105 to 75%) in the synthesis of bio-oil-phenol-formaldehyde resol resins. When the  
106 proportion of bio-oil is increased, the average molecular weight of the resin increases.  
107 Novolac resin is almost unable to crosslink without a curing agent, which is allowed  
108 to modify the novolac resin by melt blending with flexible thermoplastic polymers. In  
109 order to improve the toughness of novolac resin, some curing agents were proposed.  
110 Hexamethylenetetramine (HMTA), which provides a source of formaldehyde, was the  
111 most traditional curing agent of novolacs, but it also has environmental concerns, as it

112 is susceptible to decomposition into ammonia and formaldehyde upon heating [5, 6, 8,  
113 17, 18]. Therefore, HMTA can be replaced with an environment friendly curing  
114 agents, such as epoxy, glyoxal, oxazolidine, solid resole, resorcinol, tannin,  
115 organosolv lignin, and Kraft lignin [5, 19]. Among these curing agents, the cure  
116 reaction of the biphenyl epoxy/phenol novolac resin system has been studied by many  
117 scholars [20-22]. Novolac type phenolic resin was usually used as the curing agent of  
118 epoxy resin by making use of the OH-epoxy reaction to produce low moisture  
119 absorbing and void-free products for various electronic applications [23]. In addition,  
120 Zhang et al. [24] used glucose to prepare a sustainable novolac-type phenol-  
121 hydroxymethylfurfural (PHMF) resin. Bisphenol A diglycidyl ether (DGEBA) was  
122 used as a formaldehyde-free curing agent. By observing the kinetic parameters  
123 obtained from differential scanning calorimetry (DSC), DGEBA resin proved to be an  
124 effective cross-linker for curing PHMF by comparing it to HMTA [24].

125 In our previous work [15, 25], we used a drop tube reactor to produce beechwood bio-  
126 oil, which was then condensed in a three-stage condensation system (temperature set  
127 as 110, 20 and -11 °C) to obtain three fractions of bio-oil. Based on both separation  
128 and purification methods, many kinds of phenol rich bio-oil precursors can be chosen  
129 by using: (1) the whole bio-oil to substitute petroleum-derived phenol, (2) the bio-oil  
130 obtained from fractional condensation, or (3) the water-insoluble fractions of the bio-  
131 oil obtained from fractional condensation. In this study, the polymerization of phenol  
132 models (phenol, o-cresol, 2,6-dimethylphenol, m-cresol, and 4-ethylguaiacol) were  
133 studied to produce novolac model phenol acetaldehyde (MPA) resins. The mimic  
134 phenolics based on the composition of phenolic compounds in bio-oil were studied to  
135 produce novolac mimic acetaldehyde (mimic) resin. Bio-oil products obtained from  
136 intermediate pyrolysis of biomass were added to synthesize bio-oil acetaldehyde

137 (BOA) resins. DGEBA was used for the first time as a formaldehyde-free cross-linker  
138 for bio-oil based novolac resins. The kinetic parameters of the curing reaction with  
139 model-free methods using data obtained from DSC were determined. The  
140 physicochemical and thermal properties of MPA, mimic, and BOA resins before and  
141 after curing were compared, and the potential of bio-oil products obtained from  
142 fractional condensation and water extraction to effectively replace commercial  
143 phenols was demonstrated.

## 144 2. Experimental section

### 145 2.1. Materials

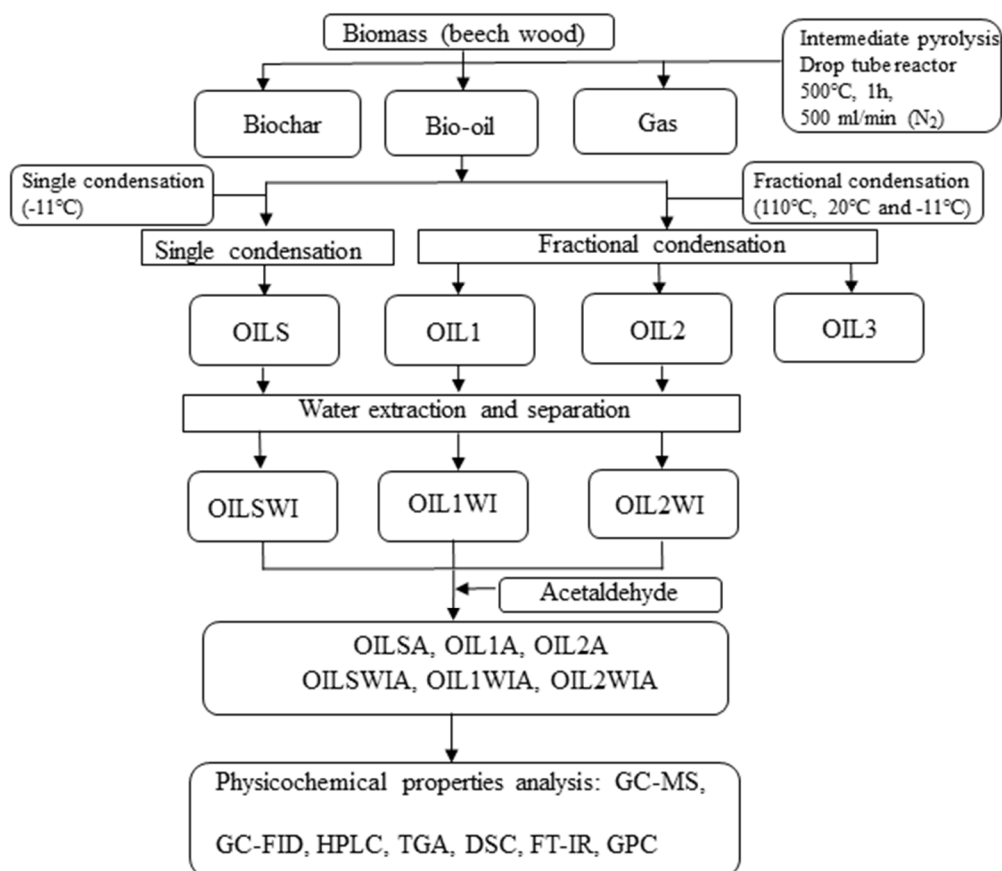
146 Bio-oil was produced by the intermediate pyrolysis of beech wood (ETS Lignex  
147 Company) in a drop tube reactor and a three-stage condensation system. The three  
148 fractions of bio-oil, named OIL1, OIL2, and OIL3, were obtained at the condensation  
149 temperature of 110, 20 and -11 °C, respectively. A single condensation condenser  
150 (temperature set at -11 °C) was used to produce a pyrolysis oil product (OILS) under  
151 the same conditions for comparison. The water-insoluble fractions (OILSWI, OIL1WI  
152 and OIL2WI) were collected by simply adding water (70 wt %) followed by  
153 centrifugation at 4000 rpm for 20 min. Based on our previous study, since OIL3  
154 mainly contains water and acids, and a very small amount of phenols [25], it did not  
155 participate in the experiments of water extraction and resin synthesis. The selected  
156 bio-oils for resin polymerization precursors are: OILS, OIL1, OIL2, OILSWI,  
157 OIL1WI and OIL2WI.

158 Phenol (99%), o-cresol (99+%), m-cresol ( $\geq 98\%$ ), 4-ethylguaiacol ( $\geq 98\%$ ), 2,6-  
159 dimethylphenol ( $\geq 99\%$ ), acetaldehyde (99%, GC), HCl (37%), methanol ( $\geq 99.8\%$ ,  
160 HPLC grade), ethanol ( $\geq 99.8\%$ , HPLC grade), acetone ( $\geq 99\%$ ), potassium hydroxide  
161 (KOH), pyridine ( $\geq 99.5\%$ , GC), dichloromethane (DCM) ( $\geq 99.8\%$ , HPLC grade),

162 acetic anhydride ( $\geq 99\%$ ), diglycidyl ether of bisphenol A (DGEBA) ( $\geq 99\%$ ), and  
 163 triphenylphosphine (TPP) ( $\geq 95.0\%$ ) were purchased from Sigma Aldrich and used as  
 164 received.

## 165 2.2. Synthesis of novolac resins

166 Polymerization tests of different phenolic precursors with acetaldehyde were carried  
 167 out. Phenol models, including phenol, o-cresol, 2,6-dimethylphenol, m-cresol, and 4-  
 168 ethylguaiacol, were used alone and named as phenol acetaldehyde (PA), o-cresol  
 169 acetaldehyde (OCA), 2,6-dimethylphenol acetaldehyde (DPA), m-cresol acetaldehyde  
 170 (MCA), and 4-ethylguaiacol acetaldehyde (EGA) resin, respectively. A mimic  
 171 phenolic resin, consisting of the above five model phenols was studied as a reference  
 172 of bio-oil to produce a mimic phenol acetaldehyde resin (mimic resin).



173

174

Fig. 1. The overview procedure of the bio-oil phenol resin synthesis and analysis

175 The molar fraction of phenol models in mimic was based on the composition of these  
 176 phenol compounds of the OIL1WI fraction, as shown in Table 1. Bio-oil products,  
 177 including OILS, OIL1, OIL2, OILSWI, OIL1WI, and OIL2WI, were also used as the  
 178 phenol precursors to synthesize BOA resins, which have different phenolic  
 179 compounds concentration.

180 Fig. 1 shows the overview of the bio-oil phenol resin procedure. Table 1 shows the  
 181 molar fraction (mol.%) of the major phenolic compounds in the bio-oil products and  
 182 the total concentration of the phenolic compounds in each product which prepared for  
 183 the bio-oil synthesis calculations.

184

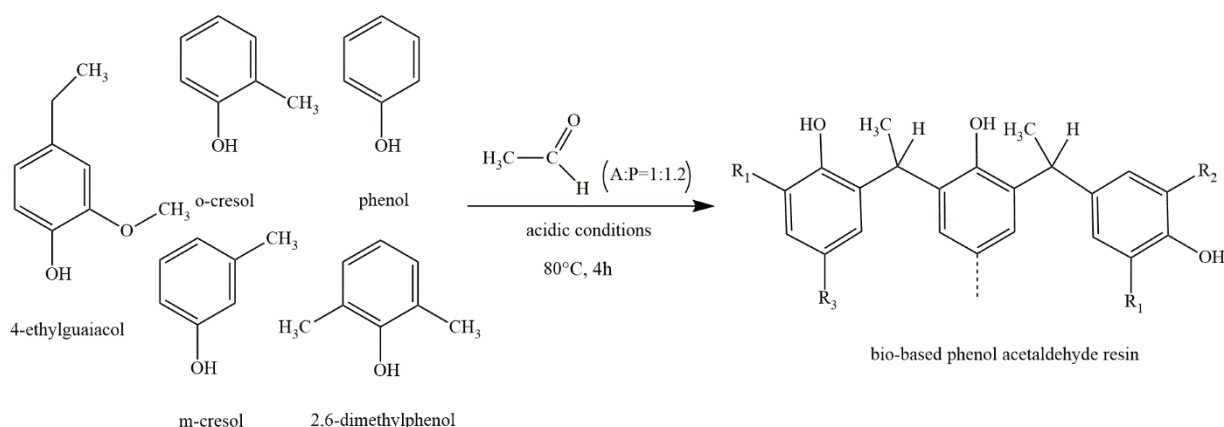
185 Table 1. Molar fraction (mol.%) determined by GC-FID for the detected phenolic compounds in oil and  
 186 the mimic composition (Average of triplicate runs with standard deviation < 3%)

| Phenols in oil                              | mol. % |      |      |        |        |        |       |
|---|--------|------|------|--------|--------|--------|-------|
|   | OILS   | OIL1 | OIL2 | OILSWI | OIL1WI | OIL2WI | mimic |
| phenol                                      | 1.03   | 1.20 | 1.21 | 3.45   | 2.47   | 2.26   | 19.73 |
| o-cresol                                    | 0.35   | 1.20 | 1.23 | 1.40   | 3.26   | 1.32   | 26.04 |
| m-cresol                                    | 0.63   | 0.94 | 0.60 | 3.23   | 1.91   | 1.33   | 15.26 |
| 2,6-dimethylphenol                          | 0.65   | 1.10 | 0.63 | 2.41   | 1.86   | 2.39   | 14.87 |
| 2,4-dimethylphenol                          | 1.25   | 3.59 | 1.04 | 4.02   | 5.06   | 4.96   | -     |
| phenol, 3-ethyl-5-methyl-                   | 0.47   | 1.00 | 0.39 | 2.46   | 2.42   | 3.03   | -     |
| 3-methylcatechol                            | 0.34   | 2.62 | 0.31 | 1.89   | 2.57   | 1.23   | -     |
| catechol                                    | 0.87   | 2.88 | 0.47 | 1.61   | 3.14   | 0.68   | -     |
| 4-methylcatechol                            | 0.43   | 1.88 | -    | 1.83   | 3.08   | -      | -     |
| 4-ethylcatechol                             | 0.47   | 1.69 | -    | 1.80   | 5.52   | -      | -     |
| guaiacol                                    | 0.82   | -    | 0.61 | 3.86   | -      | 2.87   | -     |
| creosol                                     | 0.44   | 1.69 | 0.34 | 2.00   | 3.58   | 1.83   | -     |
| 4-ethylguaiacol                             | 0.43   | 1.59 | -    | 1.80   | 3.02   | -      | 24.12 |
| syringol                                    | 0.63   | 3.06 | 0.51 | 2.70   | 4.71   | 1.97   | -     |
| isoeugenol                                  | 0.45   | 1.55 | -    | 1.78   | 3.21   | 1.30   | -     |
| 2,4-dimethoxyphenol                         | 0.30   | 1.30 | -    | 1.26   | 4.62   | 0.95   | -     |
| Phenol concentration /mmol. g <sup>-1</sup> | 1.55   | 2.69 | 1.11 | 4.23   | 5.80   | 4.03   | 8.66  |

187

188 All the resin synthesis experiments were started at atmospheric pressure. The resin  
 189 schematic of the synthesis is shown in Fig. 2. The reaction was done in a 100 mL  
 190 three-neck reactor with an oil bath preheated to a fixed temperature (80 °C) and

191 stirred with a magnetic stirrer. The reactor was equipped with a condenser and  
 192 nitrogen outlet in the middle neck, a nitrogen inlet, and a thermometer in two side  
 193 necks, respectively. After the phenol precursors melted, hydrochloric acid (HCl) was  
 194 added to obtain acidic conditions (1 mol.% HCl for phenol precursors for MPA and  
 195 mimic resins, 10 mol.% HCl for phenol precursors for BOA resins). An aldehyde to  
 196 phenol precursors molar ratio was 1:1.2, fixed for each experiment. Acetaldehyde was  
 197 then added drop-wise through the addition funnel. The reaction mixture was heated  
 198 for 4 h with continuous stirring. After the reaction, the resin products were washed  
 199 with distilled water three times and vacuum dried at 125 °C for 24 h to remove the  
 200 unreacted monomer and acid. **Each experiment was repeated three times, and the**  
 201 **average values of all the analysis were reported.**



202 **Fig. 2. Chemical structures of the phenol models (phenol, o-cresol, 2,6-dimethylphenol, m-cresol, and**  
 203 **4-ethylguaiaicol) and schematic of bio-based phenol acetaldehyde resin**

204

## 205 2.3. Characterizations

### 206 2.3.1. Determination of conversion of reactant and yield of resin

207 The resin products after drying were weighed to determine the yield, which was  
 208 calculated according to the following equation.

$$209 \text{ Yield (\%)} = \frac{\text{weight of final resin}}{\text{weight of reactant added}} \times 100 \quad (1)$$

210 The conversion rate of phenols in the polymerization reaction was calculated by Eq. 2.

$$211 \quad \text{Conversion (\%)} = \frac{\text{Mole of reactant converted}}{\text{Mole of reactant added}} \times 100 \quad (2)$$

212 Two gas chromatography instruments were used to analyze the products: a gas  
213 chromatograph-mass spectrometer instrument GC-MS (PERKIN ELMER Clarus  
214 580/SQ8S) and NIST library to identify the phenol peaks and gas chromatography  
215 with flame ionization detector GC-FID (Scion 456-GC Bruker instrument) to quantify  
216 the components. The column was a VF-1701ms (Agilent) (60 m × 0.25 mm × 0.25  
217 μm film thickness). The temperature setting procedure of the column and test method  
218 was based on our previous study [25]. Pure reference phenolic compounds were used  
219 for calibration. Standard solutions of each phenolic compound were prepared by  
220 dissolving them in acetone. Five-point straight line calibration curves (with R<sup>2</sup> > 0.99)  
221 were established for these pure compounds using nonane as the internal standard.

222

### 223 2.3.2. HPLC

224 A high-performance liquid chromatography (HPLC) instrument Agilent 1100 was  
225 used to quantify the phenolic oligomers in the MPA resins. Gradient conditions were  
226 used: 50/50 methanol/water and then 100% methanol in 20 min, back to 50/50 in 0.5  
227 min and for 5 min, a temperature of 30 °C, a flow rate of 1 ml/min, and a Kinetex  
228 C18 250 mm × 4.6 mm × 5 μm column. The detector was set at 280 nm. For  
229 identification of the oligomers, Liquid chromatography-mass spectrometry analysis  
230 was done with ISQ Single Quadrupole Mass Spectrometer from Thermo Scientific.  
231 Electrospray ionization (ESI) was used in negative mode.

232

### 233 2.3.3. ATR-FTIR

234 Attenuated total reflection Fourier-transform infrared (ATR-FTIR) spectroscopy was  
235 used to confirm the appearance of the organic functional group present in the resin  
236 samples. A SHIMADZU IRTracer-100 spectrometer with a resolution of 4 cm<sup>-1</sup> was  
237 used for analyzing the prepared samples. The spectrum was developed in reflectance  
238 mode with a wavenumber range of 450–4000 cm<sup>-1</sup>.

239

#### 240 2.3.4. Hydroxyl number

241 The hydroxyl number of the MPA, mimic, and BOA resins was measured by the  
242 titration method [26], the number of hydroxyl groups determines the crosslinking  
243 ability of the resin, which is also a very important characteristic of the novolac resin.

244 In a 250 mL round-bottom flask equipped with a condenser and a magnetic stirring  
245 bar, 0.54 g of resin sample was mixed with 10 mL of acetylation mixture (1 V acetic  
246 anhydride and 10 V pyridine). The mixture was heated at 95 to 100 °C for 60 min. 2  
247 mL of distilled water was then added. After 5 min, the funnel and neck of the flask  
248 were washed with 70 mL of cold water, which was then and collected into the flask. A  
249 blank was run under same condition without adding a resin sample. The resin sample  
250 and blank solution were titrated with a 0.5 mol/L potassium hydroxide ethanol  
251 solution using a pH meter to follow the pH value of the solution until the pH = 13.  
252 The hydroxyl number (OHN) was calculated by using Eq. 3.

$$253 \quad OHN = \frac{(V_b - V_s) \times C_{KOH}}{m_s} \quad (3)$$

254

255 V<sub>s</sub> = Consummated volume (ml) of 0.5 mol/L potassium hydroxide solution in the main test

256 V<sub>b</sub> = Consummated volume (ml) of 0.5 mol/L potassium hydroxide solution in the blank test

257 C<sub>KOH</sub> = The molar concentration of 0.5 mol/L potassium hydroxide solution

258 m<sub>s</sub> = Sample weight (g)

259

260 2.3.5. Gel permeation chromatography (GPC)

261 Molecular weight distribution was monitored by gel permeation-chromatography by  
262 a Waters Breeze gel permeation chromatography (Waters, Milford, MA, 1525 binary  
263 HPLC pump, RI detector at 270 nm, Waters Styrange HR1 column at 40 °C) with  
264 DCM as the eluent at a flow rate of 1 mL/min and polystyrene as the calibration  
265 standard. To improve the solubility of resins in the DCM solvent, all of the resin  
266 samples were subjected to acetylation by the dissolution of 0.2 g of resin in 10 mL of  
267 a mixture (1: 1 v/v) of pyridine and acetic acid followed by magnetic stirring at room  
268 temperature for 24 h. The acetylated products were obtained by precipitation in an  
269 ice-cooled 1.0 wt% HCl solution and then filtered, rinsed thoroughly with distilled  
270 water until pH = 7, and vacuum-dried at room temperature for 12 h [16].

271

272 2.3.6. Differential scanning calorimetry

273 The thermal behavior and stability of the resins was conducted on a differential  
274 scanning calorimetry (DSC) TA Q1000 instrument using about 5 mg of sample in a  
275 sealed hermetic pan and nitrogen purge gas at 50 mL/min. Samples were cycled  
276 between 25 and 180 °C at a heating/cooling rate of 5 °C/min. After that, the glass  
277 transition temperature ( $T_g$ ) was measured.

278

279 2.3.7. Thermogravimetric analysis

280 Thermogravimetric analysis (TGA) was used to monitor the thermal degradation of  
281 the uncured and cured resin. By using a TA Q600 TGA instrument, all the samples  
282 (5–10 mg) were analyzed with a heating rate of 10 °C/min from room temperature to  
283 900 °C and a 5 min plateau at 105 °C.

284

## 285 2.4. Curing treatment

286 The curing kinetics of the model phenol, mimic, and OIL1WIA resins were also  
287 studied using DSC. Firstly, the vacuum dried resin samples were dissolved in acetone  
288 and uniformly mixed with a certain percentage of the curing agent DGEBA and 2%  
289 TPP at room temperature for 12 h to evaporate all the solvent. Then, a sample of 4–5  
290 mg of the mixture was placed in an aluminum hermetic crucible and heated in a  
291 nitrogen environment from 25 °C to 250 °C at various heating rates to obtain the  
292 heating cycles. The onset temperature of curing and curing energy was determined  
293 from the heating cycle. Through optimization of the amount of DGEBA, 40% of  
294 DGEBA was selected to obtain a higher  $T_g$  (97.2 °C) of the resin as well as a curing  
295 reaction with a lower onset and a lower peak temperature.

296 The resin was thermally cured in the oven after mixing it with DGEBA. The curing  
297 temperature program was set at 120 °C for 30 min, 150 °C for 30 min, and 180 °C for  
298 1 h [24].

299

## 300 **3. Results and discussion**

### 301 3.1. Model phenol resins

#### 302 3.1.1. Resin synthesis and chemical characterization

303 Model phenols (phenol, o-cresol, 2,6-dimethylphenol, m-cresol, and 4-ethylguaiacol)  
304 and mimic were selected as phenol precursors for phenolic resin synthesis, and their  
305 properties were compared. After resinification and purification, the obtained PA resin  
306 has a dark amber color. The color of the model phenol resins like OCA and MCA is  
307 close to PA, whereas the resins like DPA, EGA, and mimic are darker than PA.

308 The conversion of phenol models after 1, 2, 3, and 4 h are shown in Fig. 3.a. It is  
309 clear that the reaction of phenol, o-cresol, and m-cresol was very fast and largely

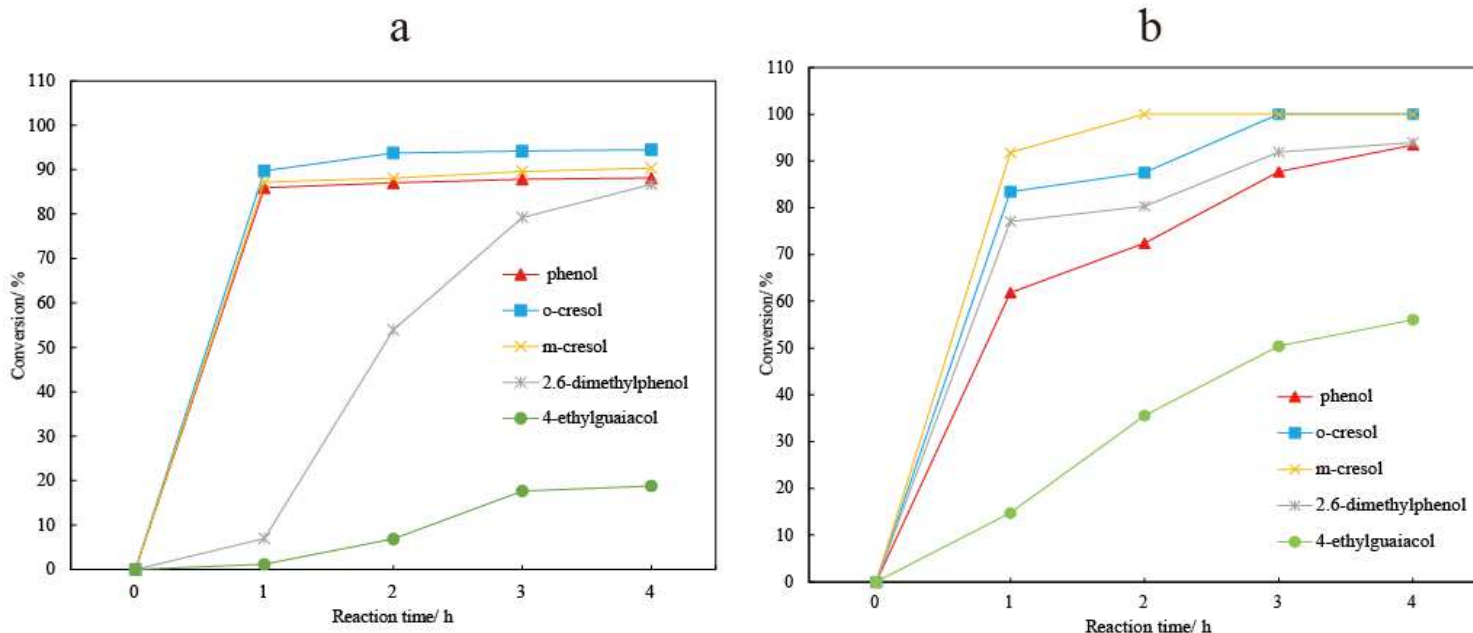
310 converted in the first hour. The final conversion was more than 88%. However, 2,6-  
 311 dimethylphenol and 4-ethylguaiacol had a relatively slower reaction, and the final  
 312 conversions were 86.70% and 18.80%, respectively. Table 2 shows the yield of the  
 313 model phenol resins. The yields of PA, OCA, and MCA are similar, whereas the yield  
 314 of DPA and EGA showed significantly lower values than the other resins. The yield  
 315 of EGA is only 15.5% due to its unreactive alkyl and methoxy groups.

316 The mimic of OIL1WI was a mixture made by these five phenol models, and the  
 317 conversion is shown in Fig. 3.b. Compared to separate reaction, phenol models in the  
 318 mimic (such as phenol, o-cresol, and m-cresol), had a relative low reaction rate in the  
 319 first hour, whereas the final conversion of them was promoted. Moreover, the  
 320 conversion of DPA and EGA increased, which indicated that the possibility of the  
 321 mutual promotion mechanism of phenolics, the cross-linking reaction of more reactive  
 322 phenols and less reactive phenols occurred. At the same time, it can be further  
 323 speculated that the polymerization reaction between the small molecules and various  
 324 phenols in the bio-oil will accelerate the overall reaction.

325 Table 2. The phenol monomer used, yield and hydroxyl number of the MPA resins

| Resin name | Phenol monomer     | Molar mass (g/mol) | Yield (wt %) | Hydroxyl number (mmol/g) | Theoretical hydroxyl number* |
|------------|--------------------|--------------------|--------------|--------------------------|------------------------------|
| PA         | phenol             | 94.11              | 82.21        | 8.56                     | 8.33                         |
| OCA        | o-cresol           | 108.14             | 82.17        | 7.67                     | 7.45                         |
| MCA        | m-cresol           | 108.14             | 83.39        | 7.78                     | 7.45                         |
| DPA        | 2,6-dimethylphenol | 122.16             | 76.06        | 6.18                     | 6.75                         |
| EGA        | 4-ethylguaiacol    | 152.19             | 15.50        | 4.41                     | 5.61                         |

326 \* Calculated from  $1000 / (\text{molecular mass of phenolic monomer} + 26)$ . 26 results from the addition of 1  
 327 molecule of acetaldehyde and the elimination of 1 molecule of water per molecule of phenolic  
 328 monomer.



329

330 Fig. 3. The conversion of a. individual phenol models during the 4 h reaction with acetaldehyde

331 b. the phenolics in the mimic resin during the 4 h reaction with acetaldehyde

332 The FTIR spectra is shown in Fig. 4 illustrated the changes in the functional groups

333 in the resins. The stretching modes at 2964, 1600, 1512, and 1450  $\text{cm}^{-1}$  of the resins

334 are attributed to the methyl group ( $-\text{CH}_3$ ), aromatic  $\text{C}=\text{C}$ , and methine ( $-\text{CH}-$ ),

335 respectively, which indicated the condensation reaction between the aldehyde in

336 acetaldehyde and the phenol to form  $-\text{CH}(\text{CH}_3)-$  linkages. All the peaks appearing

337 here illustrated the successful synthesis of the MPA resins. The absorptions at 1050

338  $\text{cm}^{-1}$  are due to  $\text{C}-\text{O}-\text{C}$  stretching, which revealed the methoxy of guaiacols, and EGA

339 showed a strong absorption here. The wide absorbance band at around 3300  $\text{cm}^{-1}$  was

340 due to  $\text{O}-\text{H}$  stretching, and the peaks located in the range of 1210  $\text{cm}^{-1}$  were assigned

341 to the  $\text{C}-\text{O}$  stretching of aromatics. Both of these peaks were assigned to the stretching

342 vibration of active phenolic hydroxy in the resin structure, and they are clear and

343 strong in all the MPA resins, whereas the peak of EGA is weaker than the others.

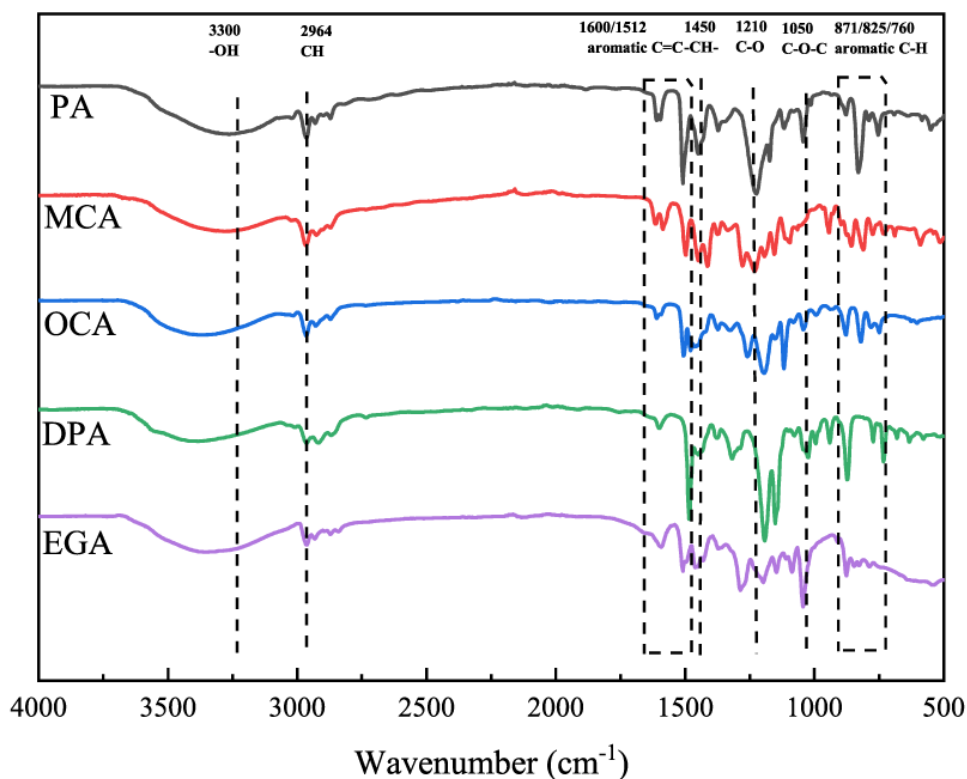


Fig. 4. FTIR graph of model phenol resins

345

346 The hydroxyl number of the resins can be more accurately quantified by titration  
 347 method is shown in Table 2. And the rank of hydroxyl number of MPA resins was:  
 348 PA > MCA > OCA > DPA > EGA. These results confirmed the results observed  
 349 in the FTIR spectra.

350 The oligomers in the resin samples were separated and identified by LC-MS [27]. As  
 351 shown in Fig. 5, the monomer, dimer, trimer, tetramer, and pentamer were separated  
 352 thoroughly and clearly were present in all the MPA resins. (2.92%, 41.99%, 24.47%,  
 353 18.51% and 12.11% for PA resin, respectively). However, the methoxy and alkyl  
 354 groups in the model phenols reduced the solubility of the oligomers in the resins. As a  
 355 result, their retention time was delayed compared with PA.

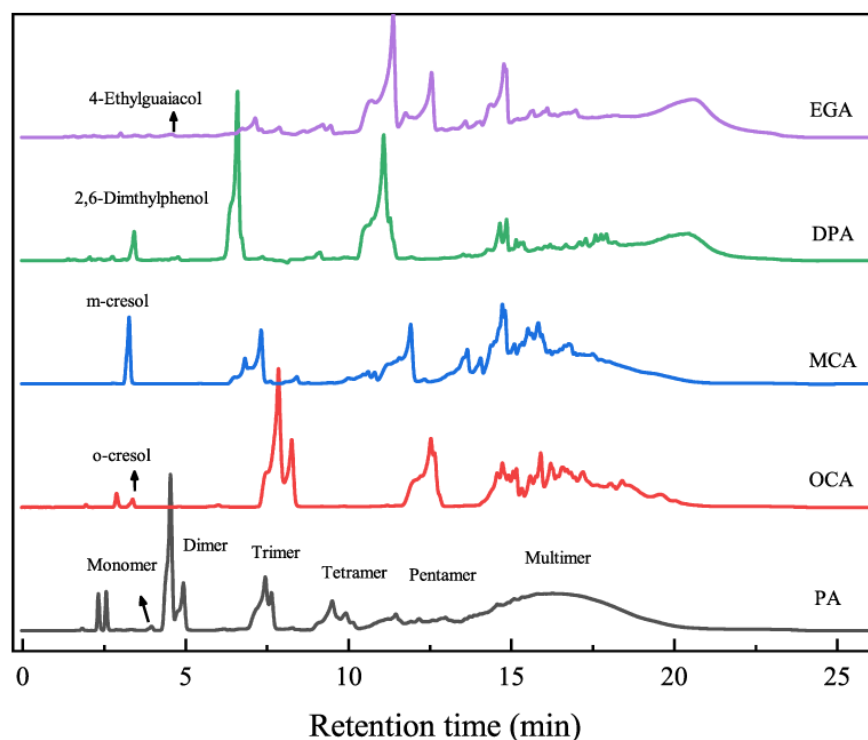


Fig. 5. Liquid chromatograms of model phenol resins.

356

357

### 358 3.1.2. Thermal Characterization of MPA resins

359 The DSC, TGA, and DTG specific results, including the glass transition temperature

360 ( $T_g$ ), the initial decomposition temperature (5% weight loss- $T_{d5}$ ), the temperature of

361 maximum decomposition rate (tallest peak of the thermogram derivative- $T_{max}$ ), and

362 the char residue formed at 800 °C ( $R_{800}$ ), were determined and are presented in Table

363 3.

364 The  $T_g$  values of the novolac resins are in the range of 44 to 68 °C. A big difference

365 between the MPA resins was observed; in particular, PA has the largest  $T_g$  value

366 (67.7 °C). The low degree of polymerization decided the relatively low  $T_g$  value of

367 EGA.

368 The thermal stability of the non-volatile content of the resins was also evaluated by

369 TGA. As shown in Table 3, the 5% weight loss of resin made by o-cresol, 2,6-

370 dimethylphenol, and 4-ethylguaiaicol was higher than that made by phenol.

371 Furthermore, the tallest peak of the thermogram derivative also reflected the reaction  
 372 degree of the resins. The feedstock that has more substituents on the aromatic ring is  
 373 difficult to react such as 4-ethylguaiacol and 2,6-dimethylphenol, and their  $T_{max}$  is  
 374 relatively lower (220.0 °C and 279.5 °C, respectively).

375 Table 3. Glass transition temperature ( $T_g$ ), initial decomposition temperature ( $T_{d5}$ ), the temperature of  
 376 maximum decomposition rate ( $T_{max}$ ), and char residue formed at 800 °C ( $R_{800}$ ) of the MPA resins

| Resin name | Phenol monomer     | $T_g$ (°C) | $T_{d5}$ (°C) | $T_{max}$ (°C) | $R_{800}$ (%) |
|------------|--------------------|------------|---------------|----------------|---------------|
| PA         | phenol             | 67.7       | 189.9         | 351.8          | 9.56          |
| OCA        | o-cresol           | 65.0       | 198.4         | 352.6          | 10.81         |
| MCA        | m-cresol           | 51.3       | 187.3         | 333.9          | 4.33          |
| DPA        | 2,6-dimethylphenol | 51.4       | 197.9         | 279.5          | 5.09          |
| EGA        | 4-ethylguaiacol    | 44.5       | 202.5         | 220.0          | 9.59          |

377

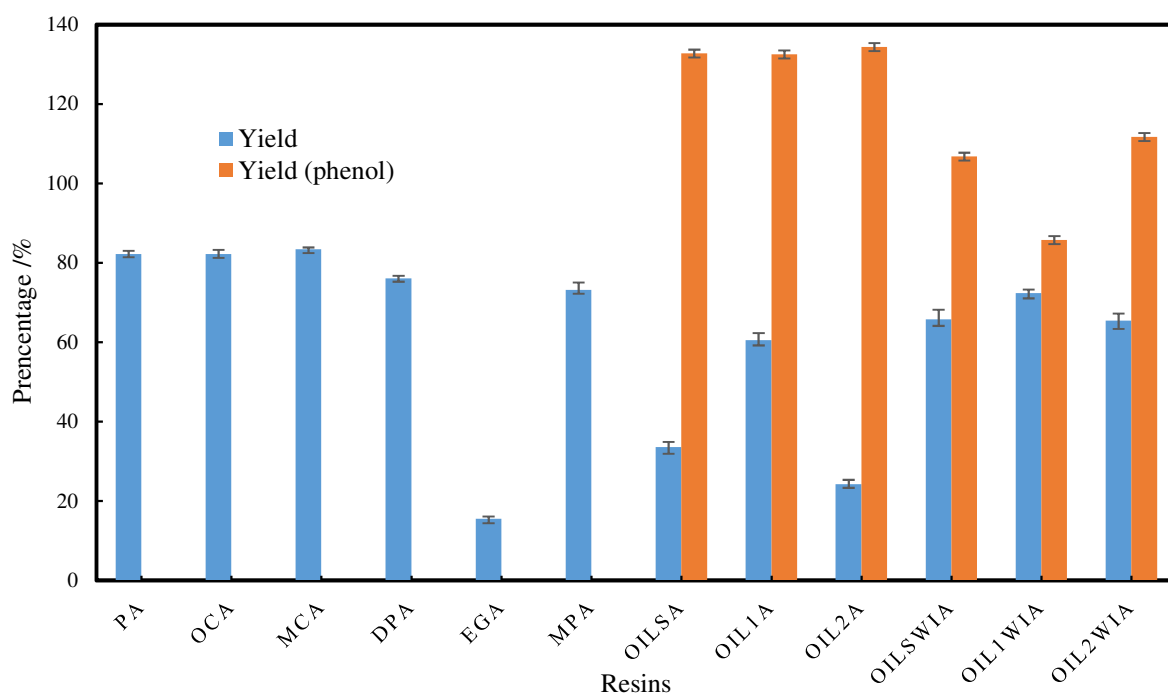
## 378 3.2. Bio-oil acetaldehyde resin

### 379 3.2.1. Resin synthesis and characterization

380 Bio-oil fractions were selected as phenol precursors for bio-oil phenolic resin  
 381 synthesis. A series of comparisons between traditional PA resin, mimic resin, and  
 382 BOA resin was carried out. After purification, the obtained mimic resin has a deep  
 383 amber color, darker than PA. All the BOA resins have a deep black color.

384 Fig. 6 shows the yield and yield by phenol for different resins based on phenol  
 385 models, mimic, and bio-oil fractions. The yield of resin reflected the degree of the  
 386 polymerization reaction. The difference between “yield” and “yield (phenol)” is based  
 387 on the calculation method of the reactant: the mass of bio-oil for “yield” and the mass  
 388 of phenols in bio-oil for “yield (phenol)”. The relationship between “yield” and “yield  
 389 (phenol)” indirectly indicated the cross-polymerization of chemical compounds other  
 390 than phenols. It is shown that the “yield (phenol)” of BOA resins is higher than that of  
 391 “yield”. This extra part of yield indicates that the cross-polymerization of compounds

392 such as aldehydes and ketones in the bio-oil took place. Correspondingly, using  
 393 fractional condensation, the bio-oil showed a higher yield (phenol) compared to the  
 394 bio-oil water-insoluble fractions as the phenol source to product phenol resin. The  
 395 water extraction step efficiently removed small reactive compounds, promoting a  
 396 larger proportion and a higher concentration of phenol compounds in the water-  
 397 insoluble fraction. Furthermore, compared with OILSWIA and OIL2WIA, the two  
 398 yields of the OIL1WIA resin are the closest, indicating that the resin properties of  
 399 OIL1WIA resin are closer to those of PA resin. The chemical compounds in the  
 400 OIL1WI and OIL1WIA resins were identified by GC/MS analysis, as shown in Fig. 7.  
 401 Phenolics were the major components identified in the OILWI. After the resinification,  
 402 most of these identified phenolics have reacted. Indeed, only a few phenolics were  
 403 detected in the OIL1WIA resin, such as phenol, 2,4-dimethyl-, phenol, 2,4,6-  
 404 trimethyl-, phenol, 3-ethyl-5-methyl-, phenol, 2,6-dimethoxy- and some newly  
 405 synthesized esters.



406 Fig. 6. The yield of PA, mimic, and BOA resins

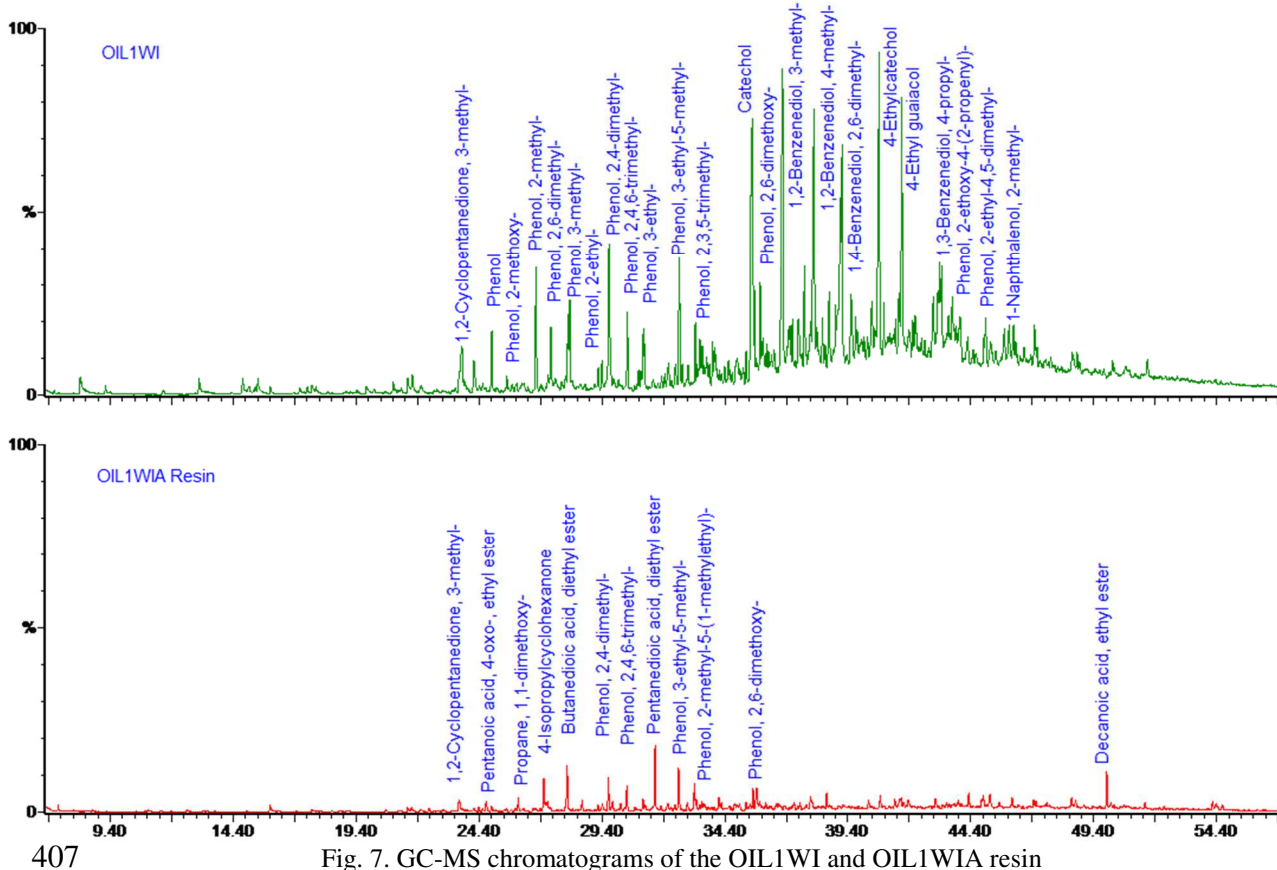


Fig. 7. GC-MS chromatograms of the OIL1WI and OIL1WIA resin

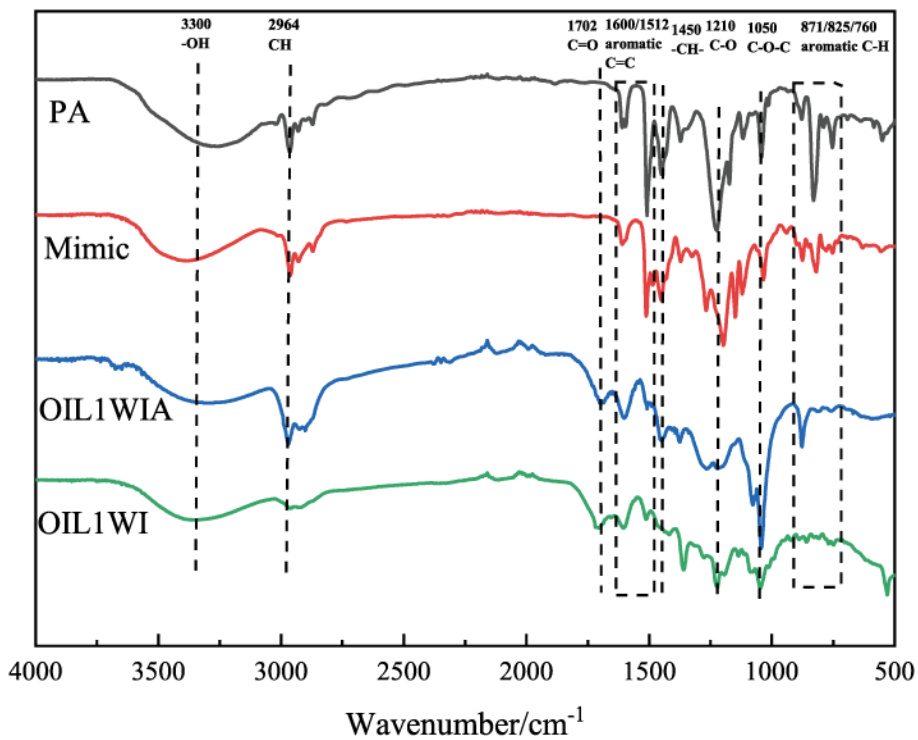
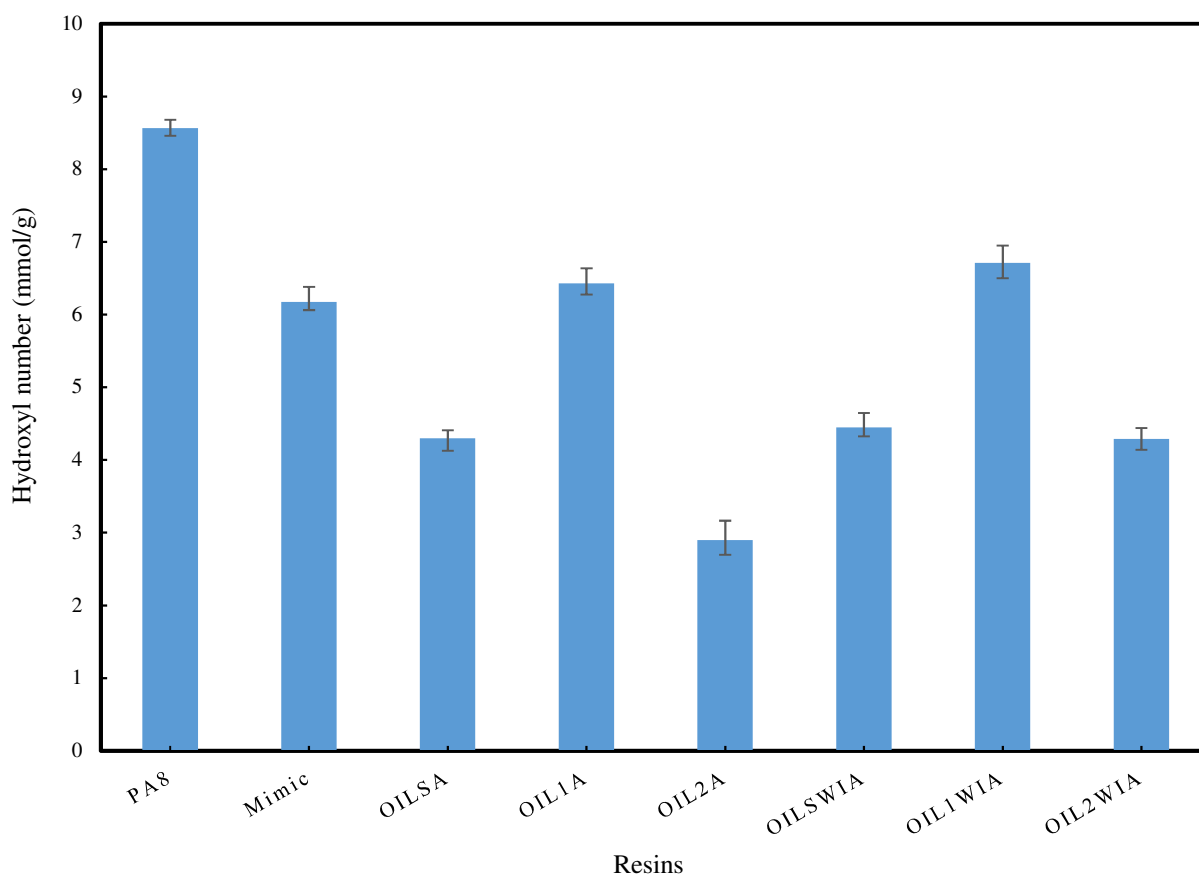


Fig. 8. FTIR graph of the PA, mimic, and OIL1WIA resin and bio-oil

409 Fig. 8 shows the FTIR spectra comparing the changes in the functional groups of the  
410 PA, mimic and OIL1WIA resins. It is obvious that the stretching at 2964, 1600, 1512,  
411 and 1450  $\text{cm}^{-1}$ , indicating the form of the  $-\text{CH}(\text{CH}_3)-$  linkages, increased in the  
412 OIL1WIA resin compared with the bio-oil (OIL1WI). The mimic, and OIL1WIA  
413 resin have strong absorption at 1050  $\text{cm}^{-1}$  due to the C–O–C stretching of guaiacols.  
414 The signals at 871, 825, as well as 760  $\text{cm}^{-1}$  were belonged to the out-of-plane  
415 bending of aromatic C–H bonds [28], and it was stronger in the PA resin than in the  
416 mimic and OIL1WIA resins. The band at 1702  $\text{cm}^{-1}$  was correlated with the aldehyde  
417 group in the bio-oil according to the incomplete separation of the families with the  
418 C=O group. The peaks at around 3300  $\text{cm}^{-1}$  and 1210  $\text{cm}^{-1}$  were assigned to the O-H  
419 and C-O of the phenolic hydroxy group in the resins. They became stronger in the PA  
420 resin than in the **mimic** resin as well as in the OIL1WIA resin. According to the  
421 titration method, the hydroxyl number of the PA and mimic resins is higher than the  
422 OIL1WIA resin, as shown in Fig. 9. Furthermore, using the water extraction fraction  
423 of the bio-oil as the phenol precursor conserved more hydroxyl groups than the  
424 untreated oil product, and OIL1WI is more suitable to produce the phenol resin  
425 among the bio-oil products to achieve characteristics approaching that of the PA resin.  
426 **It also determined the higher crosslinking ability of the OIL1WIA resin compared**  
427 **with other bio-oil based resin.**

428 The molecular weight distribution of all resins was obtained by the GPC analysis, as  
429 shown in Table 4. The GPC profiles of the OIL1WIA resin (Fig. 10) displayed a  
430 broader molecular weight distribution than that of the PA and mimic resin and had  
431 higher weight average molecular weight ( $M_w$ ) and number average molecular weight  
432 ( $M_n$ ) values ( $M_w = 3494 \text{ g/mol}$ ,  $M_n = 1136 \text{ g/mol}$ , polydispersity = 3.08). The reaction  
433 of phenols and aldehydes generally occurs in the ortho-para position of phenolic

434 hydroxyl groups, and the reactivity of phenol models decreased with the increase in  
435 the substituents [29]. Since some of the ortho and para positions of the phenolic  
436 hydroxyl groups were occupied by the methoxy group, the polymerization of 4-  
437 ethylguaiacol, for example, became more complicated due to steric hindrance. Unlike  
438 a real bio-oil which contains many small molecules and other more reactive phenols  
439 such as catechol, the composition of the mimic only contains five kinds of phenols,  
440 leading to a gap in characteristics. Hence, the phenolics in the mimic resin have fewer  
441 reactive positions per molecule than the phenol, leading to similar values of  $M_w$  and  
442  $M_n$  for the PA and mimic resin, while the molecular weight distribution of mimic  
443 resin was slightly lower than the PA resin. Presumably, there are more unreacted  
444 active sites in the mimic resin.



445

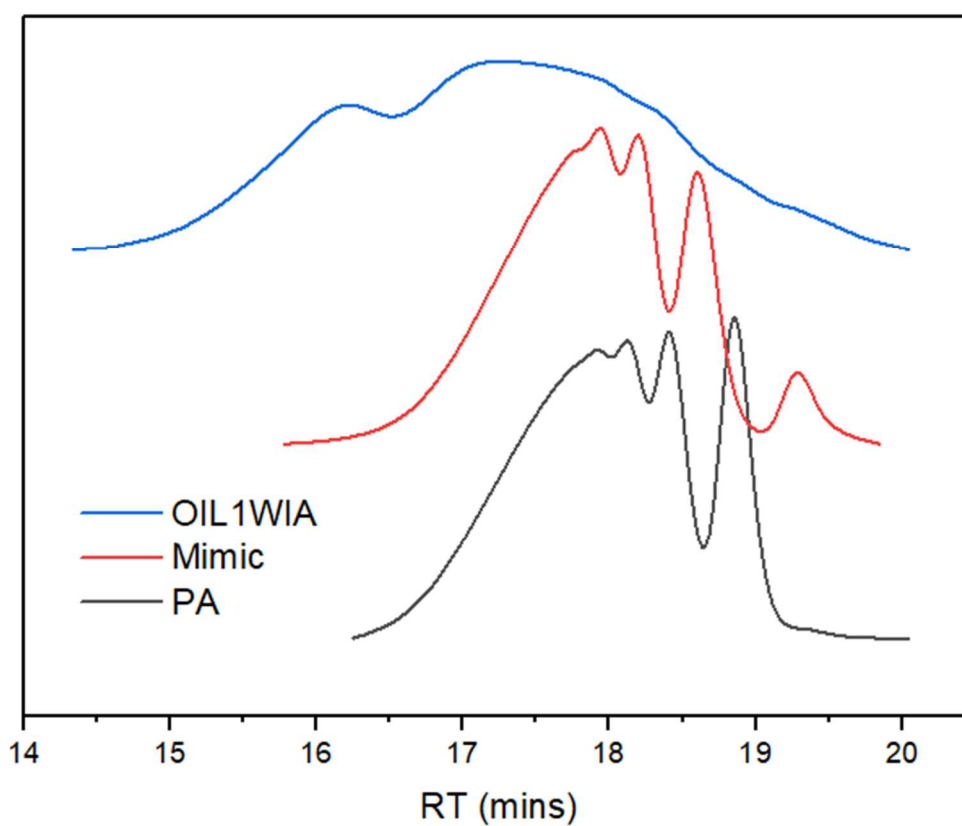
Fig. 9. The hydroxyl number of the resins

446 Table 4. GPC of the PA, mimic and OIL1WIA resin

| Resin   | M <sub>n</sub> (g/mol) | M <sub>w</sub> (g/mol) | Polydispersity |
|---------|------------------------|------------------------|----------------|
| PA      | 831                    | 1204                   | 1.45           |
| mimic   | 731                    | 1147                   | 1.57           |
| OIL1WIA | 1136                   | 3494                   | 3.08           |

447

448



449

Fig. 10. GPC chromatograms of the PA, mimic, and OIL1WIA resin

450

451 3.2.2. Thermal characterization of resins

452 The thermal analysis results from DSC, TGA, and DTG ( $T_g$ ,  $T_{d5}$ ,  $T_{max}$ , and  $R_{800}$ ) are  
 453 shown in Table 5. For clear observation and comparison, the figures of the PA, mimic,  
 454 and OIL1WIA resins are shown in Fig. 11.

455 It is clear that water extraction upgrading of the bio-oil can effectively improve the  $T_g$   
 456 value of the BOA resins (DSC). The  $T_g$  value evolves according to the following  
 457 sequence: PA > mimic > OIL1WIA resin. Moreover, the  $T_g$  of the PA and mimic  
 458 resin is clear and sharp, whereas the bio-oil resin has a relatively lower glass transition  
 459 temperature and the changes are moderate. The curve of the OIL1WIA resin is not as  
 460 stable as the other two resins, while it has a slight rise when the temperature increases.  
 461 The bio-oil contains some unreacted small compounds and phenolics, which increases  
 462 the heterogeneity, and some plasticization reactions occurred simultaneously, making  
 463 the OIL1WIA resin a very complex structure according to its molecular distribution  
 464 mentioned above [30].

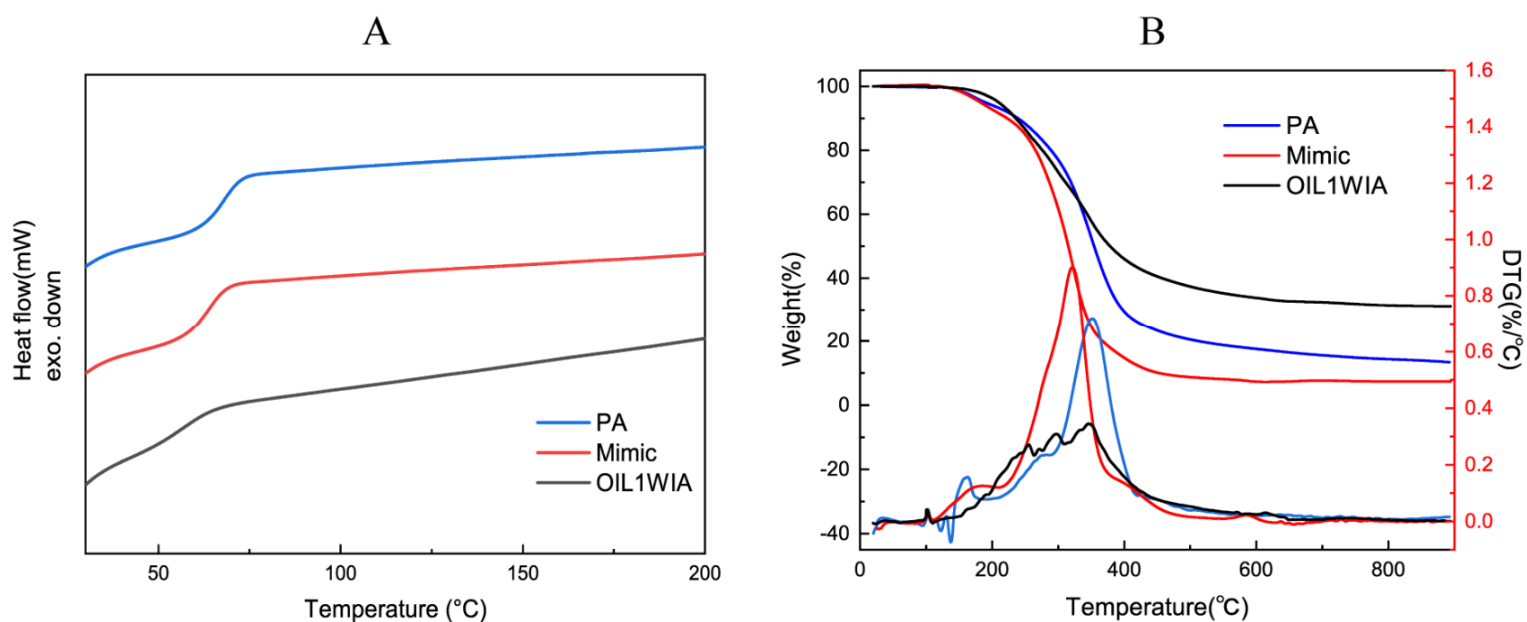
465

466 Table 5. Glass transition temperature ( $T_g$ ), initial decomposition temperature ( $T_{d5}$ ), temperature of  
 467 maximum decomposition rate ( $T_{max}$ ), and char residue formed at 800 °C ( $R_{800}$ ) of the resins

| Resin name | Phenol monomer | $T_g$ (°C) | $T_{d5}$ (°C) | $T_{max}$ (°C) | $R_{800}$ (%) |
|------------|----------------|------------|---------------|----------------|---------------|
| PA         | Phenol         | 67.7       | 189.9         | 351.8          | 9.56          |
| mimic      | Model phenols  | 63.6       | 181.6         | 338.7          | 5.62          |
| OILSA      | OILS           | 42.7       | 172.9         | 254.9          | 30.29         |
| OIL1A      | OIL1           | 43.3       | 200.0         | 291.7          | 32.24         |
| OIL2A      | OIL2           | 43.5       | 175.4         | 232.1          | 26.95         |
| OILSWIA    | OILSWI         | 58.9       | 199.7         | 332.1          | 29.35         |
| OIL1WIA    | OIL1WI         | 57.0       | 209.8         | 345.9          | 31.41         |
| OIL2WIA    | OIL2WI         | 57.3       | 205.4         | 336.4          | 30.90         |

468

469



470 Fig. 11. A. DSC, B.TG and DTG profiles of the uncured PA, mimic, and OIL1WIA resin

471 The thermal stability of the non-volatile contents of the resins was also evaluated by  
 472 TGA. As shown in Table 5, the 5% weight loss temperature of the resin made by the  
 473 bio-oil water-insoluble fractions is higher than that of the bio-oils due to their higher  
 474 reactivity demonstrated after separation. The mimic resin, which contains a large  
 475 percentage of 4-ethylguaiacol and 2,6-dimethylphenol, has a relatively small T<sub>max</sub>  
 476 compared to the PA resin due to its incomplete polymerization. The GPC result also  
 477 confirms that the molecular weight of the mimic resin is lower than that of the PA  
 478 resin. In addition, using the water extraction bio-oil fractions improved the thermal  
 479 characteristic of the resin: the OIL1WIA resin had the highest T<sub>max</sub> (345.9), which is  
 480 the closest to the PA resin among all the BOA resins. As shown in Table 5, the  
 481 residual carbon content at 800 °C for the BOA resins was higher than for the MPA  
 482 resins (comp. Table 3). This was likely caused by the cross-linking of numerous side  
 483 chains from the bio-oil molecules [30]. In summary, the OIL1WIA resin with the  
 484 feedstock of bio-oil displayed a comparable thermal resistance to that of the pure PA  
 485 resin.

486 3.3. Resin curing kinetics

487 The kinetic study of the resin curing was realized based on the DSC thermograms  
 488 obtained at different heating rates (5, 10, 15, and 20 K/min) from 25 to 250 °C. **The**  
 489 **PA, mimic, and OIL1WIA resins were cured with 40 wt% DGEBA.**  
 490 As shown in Table 6, all the temperatures of the curing reactions are between 100 and  
 491 160 °C. The mimic and BOA resins have a relatively lower initial onset temperature  
 492 compared to PA, but the ranking of the peak temperature is: mimic < PA < OIL1WIA  
 493 resin. The use of a catalyst, such as triphenylphosphine (TPP), promoted this phenol-  
 494 epoxy reaction, which is an adverse reaction. Furthermore, the chain-wise  
 495 polymerization mechanisms of the novolac/DGEBA curing system using TPP as a  
 496 catalyst included three main reaction steps: initiation, propagation, and branching [22].  
 497 The reaction mechanisms above are more adapted to the PA resin, while the reactions  
 498 of DGEBA with the mimic as well as the OIL1WIA resin are more complex due to  
 499 the existence of small compounds [20].

500 Table 6. The kinetic parameters of the PA, mimic, and OIL1WIA resin curing with 40% DGEBA

| Resin type |                 | Heating rate (K/min) |       |       |       | Activation energy (kJ/mol) |                  | n    |
|------------|-----------------|----------------------|-------|-------|-------|----------------------------|------------------|------|
|            |                 | 5                    | 10    | 15    | 20    | Kissinger                  | Flynn-Wall-Ozawa |      |
| PA         | Onset temp (°C) | 107.7                | 117.9 | 124.4 | 126.1 | 94.9                       | 96.8             | 0.95 |
|            | Peak temp (°C)  | 134.8                | 144.0 | 150.5 | 154.4 |                            |                  |      |
| Mimic      | Onset temp (°C) | 100.8                | 106.3 | 113.5 | 114.3 | 80.0                       | 82.4             | 0.94 |
|            | Peak temp (°C)  | 118.8                | 130.2 | 136.0 | 140.3 |                            |                  |      |
| OIL1WIA    | Onset temp (°C) | 100.9                | 110.8 | 119.9 | 120.5 | 95.5                       | 97.4             | 0.95 |
|            | Peak temp (°C)  | 138.4                | 147.5 | 154.8 | 157.8 |                            |                  |      |

501

502 The non-isothermal DSC analysis is widely applied to study the curing behavior and  
 503 kinetics for resin and polymer synthesis [20, 22, 24]. The results obtained from the

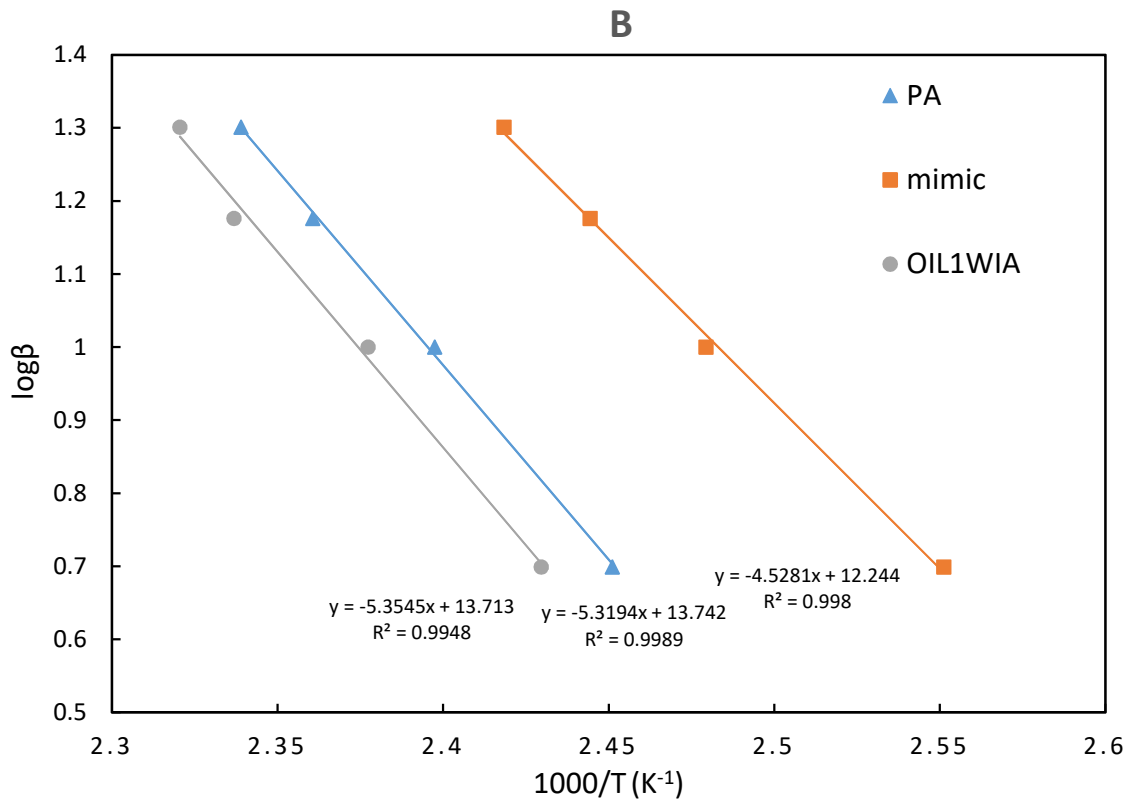
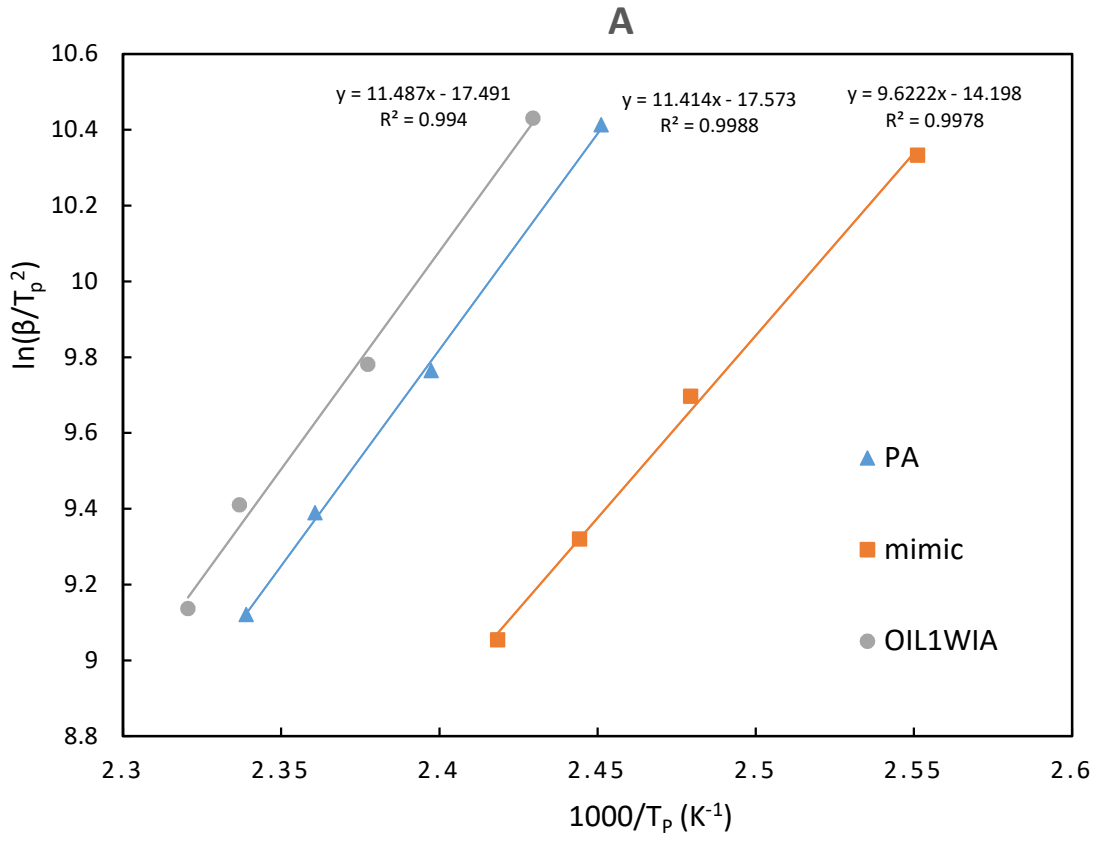
504 DSC measurements are then used to evaluate the kinetic parameters according to the  
505 model-free methods of Kissinger, Flynn–Wall–Ozawa (FWO), and Crane equations,  
506 which are illustrated by the following equations (4), (5), and (6) shown below [16, 24,  
507 31].

508 Kissinger equation 
$$\ln\left(\frac{\beta}{T_p^2}\right) = \ln\left(\frac{AR}{E_a}\right) - \frac{E_a}{RT_p} \quad (4)$$

509 Ozawa equation 
$$\log \beta = -\frac{0.4567E_a}{RT_p} + C \quad (5)$$

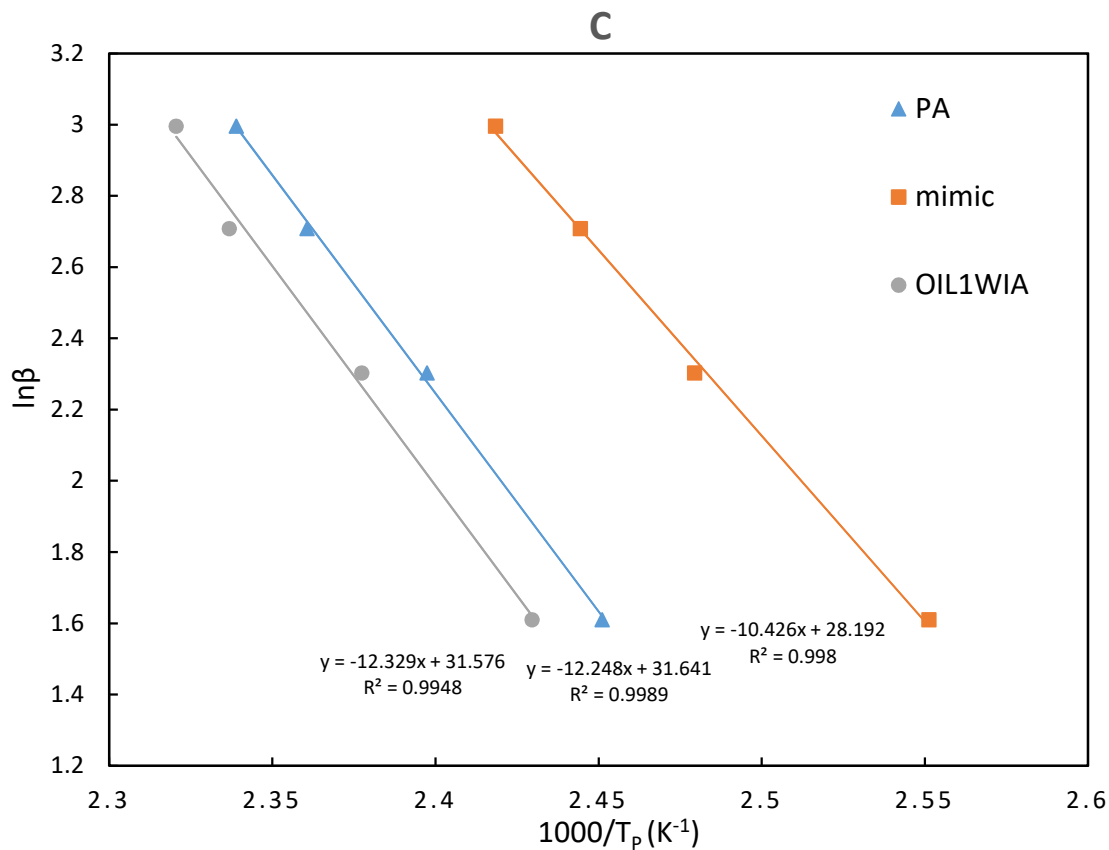
510 Crane equation 
$$\frac{d\ln\beta}{d(1/T_p)} = -\frac{E_a}{nR} \quad (6)$$

511 where  $\beta$  is the heating rate (K/min),  $T_p$  is the temperature of the maximum exothermic  
512 peak (K),  $E_a$  is the activation energy (J/mol),  $R$  is the gas constant (8.314 J/mol/K),  $A$   
513 is the pre-exponential factor ( $\text{min}^{-1}$ ),  $C$  is a constant, and  $n$  is the order of the cure  
514 reaction.  $E_a$  and  $n$  can be calculated by plotting  $\ln(\beta/T_p^2)$  against  $1/T_p$ ,  $\log \beta$  versus  
515  $1/T_p$ , and  $\ln \beta$  versus  $1/T_p$ , respectively. Table 6 and Fig. 12 show the values of  $E_a$ ,  $n$ ,  
516 and the correlation coefficient ( $R^2 > 0.99$ ). The curing reaction for all of the resins  
517 was approximately first order ( $n = 0.94 - 0.95$ ), which is following previous studies  
518 [16, 31]. **The mimic resin has the lowest value of  $E_a$  due to the lowest  $M_n$  and  $M_w$ ,  
519 based on the GPC result, which means it contains a lot of oligomers that facilitate  
520 crosslinking and curing with the epoxy groups.** Additionally, the  $E_a$  value of the  
521 OIL1WIA resin is slightly larger than that of PA; this might be because the bio-oil  
522 contains oligomers with a wide range of molecular weights, which have less  
523 unoccupied reactive sites, and it is difficult for the hydroxyl group to participate in the  
524 curing reaction [16].



525

526



527

528 Fig. 12. Plots of the DSC kinetic analysis by the (A) Kissinger, and (B) Ozawa, and (C) Crane  
 529 equations

530 Overall, the utilization of the bio-oil as a phenol alternative to produce the phenol-  
 531 acetaldehyde novolac resin can be a reasonable method to obtain a resin with a similar  
 532 curing condition.

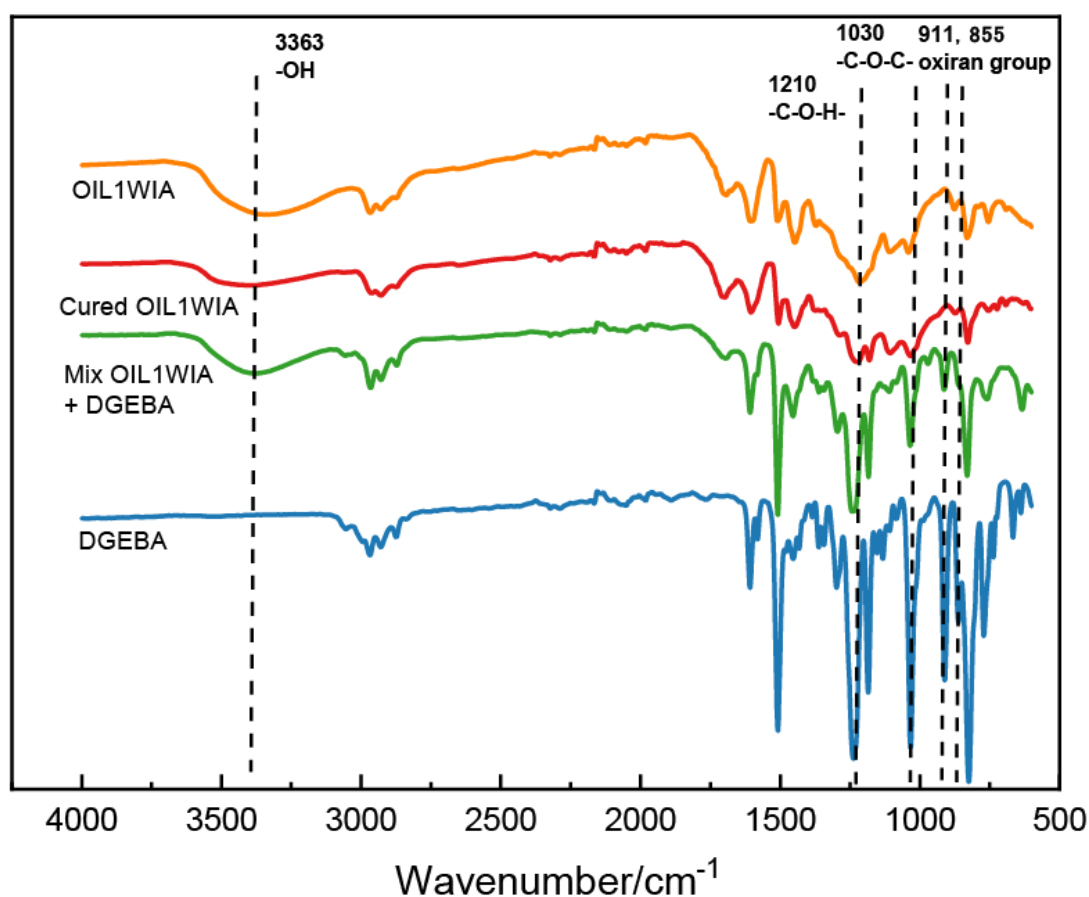
533

### 534 3.3.2 Characterization of the cured novolac resins

535 FTIR spectra were also acquired to confirm the chemical structural characterization  
 536 of the cured resin, as shown in Fig. 13. The pure DGEBA and the mixture of the  
 537 OIL1WIA resin and DGEBA were used to study the curing reaction of the OIL1WIA  
 538 resin. It is clear that the absorption band at 855 and 911 cm<sup>-1</sup> corresponding to the  
 539 characteristic peak of the oxirane ring was absent in the uncured and cured resins. In  
 540 contrast, a strong and sharp peak was observed for pure DGEBA, which decreases

541 when it is mixed with the OIL1WIA resin [32, 33]. After the curing procedure, the  
542 peak disappeared due to the reaction, indicating that almost all the epoxy groups were  
543 consumed in the curing process [34]. The increased absorption at  $1030\text{ cm}^{-1}$  was due  
544 to the C–O–C stretching, which also confirmed the presence of the ether groups in the  
545 cured resin.

546 Also, both the wide peak around  $3363\text{ cm}^{-1}$  (O–H stretching) and the peaks located in  
547 the range  $1210\text{ cm}^{-1}$  (C–O stretching) indicate the reduction of the hydroxyl group.  
548 All the changes confirmed the curing mechanism: the reaction of phenol hydroxyl and  
549 the epoxy groups, as mentioned above.



550 Fig. 13. FTIR spectra of the uncured OIL1WIA resin, cured OIL1WIA resin, the mixture of the  
551 OIL1WIA resin and DGEBA, and DGEBA

552 Thermal stability is very important as a performance criterion of the cured resin and  
 553 will ultimately affect its application value. The thermal stability of resins cured with  
 554 40% DGEBA was studied (Table 7). Compared to the thermal stability of the novolac  
 555 resin, a significant improvement was obtained after curing. At the same DGEBA  
 556 content, the cured PA, mimic, and OIL1WIA resin showed the initial and highest  
 557 thermal decomposition temperature and char yield at 800 °C after curing. However,  
 558 the trend of the initial thermal decomposition temperature of cured resins had some  
 559 differences compared with the uncured one in that the  $T_d$  (5%) of the PA and mimic  
 560 resin is higher than the OIL1WIA resin. Through curing, all resins are more stable,  
 561 and the increase in the residue also explains the occurrence of cross-linking reactions.

562 Table 7. Initial decomposition temperature ( $T_{d5}$ ), the temperature of maximum decomposition rate  
 563 ( $T_{max}$ ), and char residue formed at 800 °C ( $R_{800}$ ) of the cured resins

| Resin   | $T_{d5}$ (°C) |       | $T_{max}$ (°C) |       | $R_{800}$ (%) |       |
|---------|---------------|-------|----------------|-------|---------------|-------|
|         | uncured       | cured | uncured        | cured | uncured       | cured |
| PA      | 189.9         | 323.5 | 351.8          | 422.0 | 9.6           | 12.0  |
| mimic   | 181.6         | 294.0 | 338.7          | 414.5 | 5.6           | 11.5  |
| OIL1WIA | 209.8         | 275.3 | 345.9          | 389.6 | 31.4          | 34.4  |

564

#### 565 4. Conclusion

566 The polymerization of acetaldehyde with phenol models, mimic, and bio-oil products  
 567 from fractional condensation (OIL1 and OIL2) and water extraction (OIL1WI and  
 568 OIL2WI) were all successful, as confirmed by FTIR spectra, HPLC, GPC, and GC  
 569 analysis. The improved thermal stability of the DGEBA cured OIL1WIA resin

570 demonstrated the potential feasibility of using pyrolysis oil upgraded by water  
571 extraction to replace commercial phenol for producing a bio-based green material.

572 The relationship between “yield” and “yield (phenol)” indirectly indicated that  
573 additional cross-polymerization occurred when bio-oil is used as a phenol precursor.  
574 Among all the BOA resins, the “yield” and “yield (phenol)” of pyrolysis bio-oil from  
575 the high-temperature condenser obtained by fractional condensation and water  
576 extraction (OIL1WIA) are closer and its yield is closer to that of PA than the other  
577 resins thanks to its high content of phenolic compounds. OIL1WIA resin has thermal  
578 properties close to the PA resin.

579 DSC and FTIR analysis put in evidence that the more environmentally friendly and  
580 effective curing agent, bisphenol A type epoxy (DGEBA), was used efficiently as  
581 formaldehyde-free cross-linker for bio-oil based phenol resins. The curing of the  
582 OILWIA resin and DGEBA started earlier than the PA resin (100.9 and 107.7 °C),  
583 whereas the peak temperature has an opposite tendency at around 134.8 and 138.4 °C.  
584 The curing activation energy ( $E_a$ ) of PA and OIL1WIA resin are close.

585

## 586 **Acknowledgments**

587 This work was supported by China Scholarship Council (CSC) and the UT-INSA  
588 program between China and France. For the analytical part, this work has been  
589 partially supported by the University of Rouen Normandy, INSA Rouen Normandy,  
590 the Centre National de la Recherche Scientifique (CNRS), European Regional  
591 Development Fund (ERDF) N° HN0001343, Labex SynOrg (ANR-11-LABX-0029),  
592 Carnot Institute I2C, the graduate school for research XL-Chem (ANR-18-EURE-  
593 0020 XL CHEM) and by Region Normandie. GC/FID was financed by FEDER RIN

594 Green Chem 2019NU01FOBC08 N° 17P04374 and GC/MS by RIN 2019 FSP-  
595 CHEM NU01FOBC21 N° 18P03656

596

## 597 5. Reference

- 598 [1] J.S. Kim, Production, separation and applications of phenolic-rich bio-oil--a review,  
599 *Bioresour. Technol.* 178 (2015) 90-98.
- 600 [2] C. Mohabeer, L. Abdelouahed, S. Marcotte, B. Taouk, Comparative analysis of pyrolytic  
601 liquid products of beech wood, flax shives and woody biomass components, *J. Anal. Appl.*  
602 *Pyrolysis* 127 (2017) 269-277.
- 603 [3] J. Wang, L. Abdelouahed, J. Xu, N. Brodu, B. Taouk, Catalytic Hydrodeoxygenation of  
604 Model Bio - oils Using HZSM - 5 and Ni<sub>2</sub>P/HZM - 5 Catalysts: Comprehension of Interaction,  
605 *Chem. Eng. Technol.* 44(11) (2021) 2126-2138.
- 606 [4] X. Hu, M. Gholizadeh, Progress of the applications of bio-oil, *Renew. Sustain. Energy Rev*  
607 134 (2020).
- 608 [5] L. Pilato, *Phenolic resins: a century of progress*, Springer2010.
- 609 [6] M.H. Choi, H.Y. Byun, I.J. Chung, The effect of chain length of flexible diacid on  
610 morphology and mechanical property of modified phenolic resin, *Polymer* 43(16) (2002)  
611 4437-4444.
- 612 [7] W. Yang, L. Jiao, X. Wang, W. Wu, H. Lian, H. Dai, Formaldehyde-free self-polymerization  
613 of lignin-derived monomers for synthesis of renewable phenolic resin, *Int J Biol Macromol*  
614 166 (2021) 1312-1319.
- 615 [8] P.R. Sarika, P. Nancarrow, A. Khansaheb, T. Ibrahim, Bio-Based Alternatives to Phenol and  
616 Formaldehyde for the Production of Resins, *Polymers* 12(10) (2020).
- 617 [9] H.L. Chum, S.K. Black, Process for fractionating fast-pyrolysis oils, and products derived  
618 therefrom, Google Patents, 1990.
- 619 [10] H.L. Chum, S.K. Black, J.P. Diebold, R.E. Kreibich, Resole resin products derived from  
620 fractionated organic and aqueous condensates made by fast-pyrolysis of biomass materials,  
621 Google Patents, 1993.
- 622 [11] A.-C. Johansson, K. Iisa, L. Sandström, H. Ben, H. Pilath, S. Deutch, H. Wiinikka, O.G.  
623 Öhrman, Fractional condensation of pyrolysis vapors produced from Nordic feedstocks in  
624 cyclone pyrolysis, *J. Anal. Appl. Pyrolysis* 123 (2017) 244-254.
- 625 [12] A.S. Pollard, M.R. Rover, R.C. Brown, Characterization of bio-oil recovered as stage  
626 fractions with unique chemical and physical properties, *J. Anal. Appl. Pyrolysis* 93 (2012) 129-  
627 138.
- 628 [13] S. Ren, X.P. Ye, Stability of crude bio-oil and its water-extracted fractions, *J. Anal. Appl.*  
629 *Pyrolysis* 132 (2018) 151-162.
- 630 [14] X. Zhang, H. Ma, S. Wu, W. Jiang, W. Wei, M. Lei, Fractionation of pyrolysis oil derived  
631 from lignin through a simple water extraction method, *Fuel* 242 (2019) 587-595.
- 632 [15] J. Xu, N. Brodu, L. Abdelouahed, B. Taouk, Investigation of the combination of fractional  
633 condensation and water extraction for improving the storage stability of pyrolysis bio-oil,  
634 *Fuel* 314 (2022).
- 635 [16] S. Cheng, I. D'Cruz, Z. Yuan, M. Wang, M. Anderson, M. Leitch, C.C. Xu, Use of biocrude  
636 derived from woody biomass to substitute phenol at a high-substitution level for the  
637 production of biobased phenolic resol resins, *J. Appl. Polym. Sci.* 121(5) (2011) 2743-2751.
- 638 [17] K. Hirano, M. Asami, Phenolic resins—100years of progress and their future, *React.*  
639 *Funct. Polym.* 73(2) (2013) 256-269.

640 [18] Y. Zhang, Z. Yuan, C. Xu, Bio-based resins for fiber-reinforced polymer composites,  
641 Natural Fiber-Reinforced Biodegradable and Bioresorbable Polymer Composites 2017, pp.  
642 137-162.

643 [19] Y. Zhang, Z. Yuan, C.C. Xu, Engineering biomass into formaldehyde-free phenolic resin  
644 for composite materials, *AIChE J.* 61(4) (2015) 1275-1283.

645 [20] W.S. Choi, A.M. Shanmugharaj, S.H. Ryu, Study on the effect of phenol anchored  
646 multiwall carbon nanotube on the curing kinetics of epoxy/Novolac resins, *Thermochim.*  
647 *Acta* 506(1-2) (2010) 77-81.

648 [21] S. Han, H. Gyu Yoon, K.S. Suh, W. Gun Kim, T. Jin Moon, Cure kinetics of biphenyl  
649 epoxy - phenol novolac resin system using triphenylphosphine as catalyst, *J. Polym. Sci., Part*  
650 *A: Polym. Chem.* 37(6) (1999) 713-720.

651 [22] S.-p. Ren, Y.-x. Lan, Y.-q. Zhen, Y.-d. Ling, M.-g. Lu, Curing reaction characteristics and  
652 phase behaviors of biphenol type epoxy resins with phenol novolac resins, *Thermochim.*  
653 *Acta* 440(1) (2006) 60-67.

654 [23] C. Nair, Advances in addition-cure phenolic resins, *Prog. Polym. Sci.* 29(5) (2004) 401-  
655 498.

656 [24] Y. Zhang, F. Ferdosian, Z. Yuan, C.C. Xu, Sustainable glucose-based phenolic resin and its  
657 curing with a DGEBA epoxy resin, *J. Taiwan Inst. Chem. Engrs.* 71 (2017) 381-387.

658 [25] J. Xu, N. Brodu, J. Wang, L. Abdelouahed, B. Taouk, Chemical characteristics of bio-oil  
659 from beech wood pyrolysis separated by fractional condensation and water extraction, *J.*  
660 *Energy Inst.* 99 (2021) 186-197.

661 [26] S. Benyahya, C. Aouf, S. Caillol, B. Boutevin, J.P. Pascault, H. Fulcrand, Functionalized  
662 green tea tannins as phenolic prepolymers for bio-based epoxy resins, *Ind Crops Prod* 53  
663 (2014) 296-307.

664 [27] P. Zhang, S. Wang, X. Zhang, X. Jing, The effect of free dihydroxydiphenylmethanes on  
665 the thermal stability of novolac resin, *Polym. Degrad. Stab.* 168 (2019).

666 [28] Y. Cui, X. Hou, W. Wang, J. Chang, Synthesis and Characterization of Bio-Oil Phenol  
667 Formaldehyde Resin Used to Fabricate Phenolic Based Materials, *Materials* 10(6) (2017).

668 [29] J.F. Stanzione, P.A. Giangiulio, J.M. Sadler, J.J. La Scala, R.P. Wool, Lignin-Based Bio-Oil  
669 Mimic as Biobased Resin for Composite Applications, *ACS Sustain. Chem. Eng.* 1(4) (2013)  
670 419-426.

671 [30] A.E. Vithanage, E. Chowdhury, L.D. Alejo, P.C. Pomeroy, W.J. DeSisto, B.G. Frederick,  
672 W.M. Gramlich, Renewably sourced phenolic resins from lignin bio-oil, *J. Appl. Polym. Sci.*  
673 134(19) (2017).

674 [31] M. Wang, L. Wei, T. Zhao, Cure study of addition-cure-type and condensation–addition-  
675 type phenolic resins, *Eur. Polym. J.* 41(5) (2005) 903-912.

676 [32] Y. Celikbag, S. Meadows, M. Barde, S. Adhikari, G. Buschle-Diller, M.L. Auad, B.K. Via,  
677 Synthesis and Characterization of Bio-oil-Based Self-Curing Epoxy Resin, *Ind. Eng. Chem. Res.*  
678 56(33) (2017) 9389-9400.

679 [33] B. Sibaja, S. Adhikari, Y. Celikbag, B. Via, M.L. Auad, Fast pyrolysis bio-oil as precursor of  
680 thermosetting epoxy resins, *Polym. Eng. Sci.* 58(8) (2018) 1296-1307.

681 [34] Z. Wang, P. Gnanasekar, S. Sudhakaran Nair, R. Farnood, S. Yi, N. Yan, Biobased Epoxy  
682 Synthesized from a Vanillin Derivative and Its Reinforcement Using Lignin-Containing  
683 Cellulose Nanofibrils, *ACS Sustain. Chem. Eng.* 8(30) (2020) 11215-11223.

684